JOURNAL

OF THE AMERICAN CHEMICAL SOCIETY

VOLUME 104, NUMBER 18 SEPTEMBER 8, 1982

Kinetics of Free Radicals Produced by Infrared Multiphoton-Induced Decomposition. 2. Formation of Acetyl and Chlorodifluoromethyl Radicals and Their Reactions with Nitrogen Dioxide

Irene R. Slagle and David Gutman*

Contribution from the Department of Chemistry, Illinois Institute of Technology, Chicago, Illinois 60616. *Received February 1, 1982*

Abstract: A versatile, indirect method of producing polyatomic free radicals under conditions which are suitable for quantitative studies of their gas-phase reactions has been developed. Cl atoms are homogeneously generated in a flow reactor by the infrared multiple-photon-induced decomposition (IRMPD) of CF_2Cl_2 or C_6F_5Cl and then rapidly reacted with an organic precursor to produce the desired free radical. Reactions of this free radical can then be monitored in a time-resolved manner using photoionization mass spectrometry. In this study we have produced the acetyl radical and studied its reaction with NO_2 under pseudo-first-order conditions in order to determine not only the rate constant but also to verify the mechanism of this oxidation reaction. Modeling of reactant and product ion signal profiles indicates that the products produced and rate constants (k_4) are $CH_3CO + NO_2 \rightarrow CH_3CO_2 + NO$, with $k_4 = 2.5\ (\pm 0.6) \times 10^{-11}$ cm^3 molecule^{-1} s^{-1} at 295 K. In addition, the rate and mechanism of the reaction of CF_2Cl (produced by the direct IRMPD of CF_2Cl_2) with NO_2 have also been determined. The products produced and rate constants (k_5) are $CF_2Cl + NO_2 \rightarrow CF_2ClO + NO$ with $k_5 = 9.6\ (\pm 1.9) \times 10^{-12}$ cm^3 molecule^{-1} s^{-1}.

In order to gain new knowledge of the reactivity of gaseous polyatomic free radicals, we have recently developed a versatile new method for conducting quantitative studies of their reactions. The method involves the direct homogeneous generation of free radicals in a tubular reactor by the infrared multiple-photon-induced decomposition (IRMPD) of suitable radical precursors and the dynamic monitoring of both reactant and product concentration profiles using photoionization mass spectrometry (PIMS). The method and its initial use, a study of the reactions of allyl radicals with NO_2 and Br_2, were described in part 1.[1] A second study, involving the generation of methyl radicals and their subsequent reaction, has also been reported.[2]

The direct production of polyatomic free radicals for kinetic studies by IRMPD is proving to be an extremely versatile and useful method of homogeneously producing known concentrations of reaction intermediates for chemical kinetic studies.[1-7] However, there are instances where an indirect method (involving the initial production of chlorine atoms by IRMPD followed by a rapid Cl-atom reaction with an organic molecule) is preferable. In particular, if the laser pulse which produces the polyatomic intermediate of interest is also capable of decomposing it,[7-9] delayed production of the free radical would be an advantage. Also, if no suitable precursor for a particular intermediate has yet been identified, this more circuitous route would provide an alternate method of generating the desired free radical under conditions which are also very well characterized. We have now used such an indirect procedure to generate the acetyl radical, a free radical for which we have not yet identified a suitable precursor molecule for direct generation by IRMPD, and we have studied the mechanism and rate of its reaction with NO_2. The details of the procedure and the results of this study are reported here.

Organic free radicals have been generated by halogen-atom reactions in a variety of experimental arrangements for studies

---

(1) Slagle, I. R.; Gutman, D. *J. Am. Chem. Soc.* **1981**, *103*, 149–153.

(2) Yamada, F.; Slagle, I. R.; Gutman, D. *Chem. Phys. Lett.* **1981**, *83*, 409–412.

(3) Martinez, R. I.; Huie, R. E.; Herron, J. T.; Braun, W. *J. Phys. Chem.* **1980**, *84*, 2344–2347.

(4) Rossi, M. J.; Barker, J. R.; Golden, D. M. *J. Chem. Phys.* **1979**, *71*, 3722–3727.

(5) Golden, D. M.; Rossi, M. J.; Baldwin, A. C.; Barker, J. R. *Acc. Chem. Res.* **1981**, *14*, 56–62.

(6) Rossi, M. J.; Barker, J. R.; Golden, D. M. *Int. J. Chem. Kinet.*, in press.

(7) Rossi, M. J.; Barker, J. R.; Golden, D. M. *J. Chem. Phys.* **1982**, *76*, 406–416.

(8) Francisco, J. S.; Findeis, M. A.; Steinfeld, J. I. *Int. J. Chem. Kinet.* **1981**, *13*, 627–38.

(9) Schultz, P. A.; Sudhø, Aa. S.; Kranjovich, D. J.; Kwok, H. S.; Shen, Y. R.; Lee, Y. T. *Annu. Rev. Phys. Chem.* **1979**, *30*, 379–409.

(10) Radford, H. E.; Evenson, K. M.; Jennings, D. A. *Chem. Phys. Lett.* **1981**, *78*, 589–591.

(11) Inoue, G.; Akimoto, H.; Okuda, M. *J. Chem. Phys.* **1980**, *72*, 1769–1775.

(12) Inoue, G.; Akimoto, H. *J. Chem. Phys.* **1981**, *74*, 425–433.

(13) Niki, H.; Maker, P. D.; Savage, C. M.; Breitenbach, L. P. *J. Mol. Struct.* **1980**, *59*, 1–13.

(14) Dyke, J. M.; Jonathan, N.; Morris, A.; Winter, M. J. *Mol. Phys.* **1980**, *39*, 629–636.

0002-7863/82/1504-4741$01.25/0

of their spectroscopy,[10-14] kinetics,[15-18] and thermochemistry.[19] In our current use of these reactions, it has been possible for the first time not only to isolate the following reaction of the polyatomic free radical but also to study it under pseudo-first-order conditions in a direct time-resolved manner. Recently, similar isolation has been achieved under steady conditions in a flow reactor using chlorine atoms generated in a microwave discharge.[15]

In our experiments chlorine atoms were generated by IRMPD of either CF_2Cl_2 or C_6F_5Cl:

$$CF_2Cl_2 \xrightarrow{nh\nu} CF_2Cl + Cl \tag{1}$$

$$C_6F_5Cl \xrightarrow{nh\nu} C_6F_5 + Cl \tag{2}$$

Acetaldehyde and NO_2 were also present in the system. The chlorine atoms reacted rapidly with the acetaldehyde to produce acetyl radicals,

$$Cl + CH_3CHO \rightarrow CH_3\dot{C}O + HCl \tag{3}$$

and the acetyl radicals subsequently reacted with NO_2:

$$CH_3CO + NO_2 \rightarrow CH_3CO_2 + NO \tag{4}$$

By using suitable choices of initial concentrations, all three processes were temporally separated.

The reaction

$$CF_2Cl + NO_2 \rightarrow CF_2ClO + NO \tag{5}$$

was also studied, the CF_2Cl radicals originating from the same IRMPD process which produced the Cl atoms (reaction 1).

The bimolecular reactions of acyl radicals are involved in a variety of oxidation processes particularly during low-temperature combustion of hydrocarbons, where bimolecular reactions of these radicals, particularly with O_2, compete with their unimolecular dissociation,[20-22] and during the atmospheric photooxidation of unsaturated hydrocarbons.[23-25] Despite their importance in practical oxidation processes, few gaseous reactions of acyl radicals have been isolated for investigation.[26] The important atmospheric reactions of HCO, those with NO and O_2, as well as its self-reaction have now been studied by several groups using time-resolved absorption measurements of HCO produced by laser or flash photolysis.[27-32] Because more complex acyl radicals have significantly weaker absorption spectra, analogous studies have not yet been performed on the reactions of larger RCO radicals. An exception is studies of their recombination reactions where high initial free-radical concentrations are employed.[33,34] PIMS has already been used to monitor HCO and CH_3CO concentrations during controlled reactions.[27,35] These studies have yielded quantitative information on reactions of HCO and CH_3CO with O_2.[27,35] The latter study involved direct production of acetyl radicals by UV flash photolysis followed by time-resolved measurements of CH_3CO concentrations using a PIMS which is very similar to the one used in our studies.

We have begun a series of studies of the reactions of acyl radicals to enlarge our knowledge of their kinetics and mechanisms. The first reaction we have investigated, reaction 4, is of special interest because it is believed to produce acetoxy radical, an intermediate which is generally regarded to be highly unstable, decomposing almost instantly ($\sim 10^{-10}$ s) into CH_3 and CO_2.[36-39] Evidence for this instability originates primarily from observed cage decarboxylation of the acetoxy radical produced by flash photolysis of $(CH_3CO_2)_2$ or CH_3CO_2Br in liquids.[40-43] In smog cycle mechanisms, alkylcarboxy radicals, RCO_2, are produced by a sequence of reactions which begin with the oxidation of acyl radicals by atmospheric oxygen, e.g.,

$$CH_3CO + O_2 \rightarrow CH_3CO_3 \tag{6}$$

The acylperoxy radical may either combine with NO_2 to form peroxyacetyl nitrate (PAN) or react with NO to form the acylcarboxy radical:[23-25]

$$CH_3CO_3 + NO_2 \rightarrow CH_3CO_3NO_2 \tag{7}$$

$$\begin{gathered} CH_3CO_3 + NO \rightarrow CH_3CO_2 + NO_2 \\ CH_3CO_2 \rightarrow CH_3 + CO_2 \end{gathered} \tag{8}$$

Reaction 4 appears to be the most direct means of producing the acetoxy radical. We studied this reaction in order not only to establish its rate constant but also to provide more direct evidence for the formation of this reaction intermediate.

Experimental Section

The experimental apparatus and most procedures used were essentially the same as those described in part 1.[1] Radiation from a Lumonics 103-2 CO_2 TEA laser was mildly concentrated with a 5-m focal length concave mirror. The long beam waist was concentric with and located along the axis of the 35-cm-long, 0.95-cm i.d. tubular Pyrex reactor. Gas flowing through the reactor was irradiated with almost uniform intensity along the reactor's length at a repetition rate of 0.5 Hz. Laser fluences up to 3.5 J/cm^2 were used.

The gas flowing through the tube contained CF_2Cl_2, the Cl-atom source (usually less than 0.01%); CH_3CHO, the source of acetyl radicals ($\sim$2%); NO_2, the second reactant (0–0.02%); and a large excess of He buffer gas ($\sim$98%). The high percentage of inert gas assures negligible heating following the relaxation of the undissociated but internally excited Cl-atom source. Total gas pressures were varied from 1 to 2 torr.

Gas was continuously sampled from a 0.044-cm-diameter hole in the side of the reactor. The emerging gas was formed into a beam by a conical skimmer as it entered the vacuum chamber containing the PIMS. As the gas traversed the ion source, a portion was photoionized and mass selected by a quadrupole mass filter. In separate experiments, temporal ion signal profiles of reactants and possible products were recorded with a multichannel scalar from a period just before each laser pulse to about 50 ms following the pulse.

The new experimental procedures used in this study are discussed below.

Generation of Chlorine Atoms. Chlorine atoms were produced by IRMPD of CF_2Cl_2 at 1082 cm^{-1}. The IRMPD of CF_2Cl_2 is known to proceed to a significant extent by this route at the modest fluences used in our studies.[44-46] Very minor amounts of CF_2 were also produced

---

(15) Plumb, I. C.; Ryan, K. R. *Int. J. Chem. Kinet.* **1981**, *13*, 1011–1028.

(16) Niki, H.; Maker, P. D.; Savage, C. M.; Breitenbach, L. P. *J. Phys. Chem.* **1981**, *85*, 877–881.

(17) Nesbitt, D. J.; Leone, S. R. *J. Chem. Phys.* **1980**, *72*, 1722–1732.

(18) Sander, S. P.; Watson, R. T. *J. Phys. Chem.* **1980**, *84*, 1664–1674.

(19) Baghal-Vayjooee, M. H.; Colussi, A. J.; Benson, S. W. *Int. J. Chem. Kinet.* **1979**, *11*, 147–154.

(20) Minkoff, G. J.; Tipper, C. F. H. "Chemistry of Combustion Reactions"; Butterworths: London, 1962.

(21) Griffiths, J. F.; Skirrow, G. *Oxid. Combust. Rev.* **1968**, *3*, 47–96.

(22) Ray, D. J. M.; Ruiz-Diaz, R.; Waddington, D. J. *Symp. (Int.) Combust., [Proc.]* **1973**, *14*, 259–266.

(23) Leighton, P. A. "Photochemistry of Air Pollution"; Academic Press: New York, 1961.

(24) Demerjian, K. L.; Kerr, J. A.; Calvert, J. G. *Adv. Environ. Sci. Technol.* **1974**, *4*, 1–262.

(25) Carter, W. P. L.; Lloyd, A. C.; Sprung, J. L.; Pitts, J. N. *Int. J. Chem. Kinet.* **1979**, *11*, 45–101.

(26) Caronna, T.; Minisci, F. *Rev. React. Species Chem. React.* **1976**, *1*, 263–318.

(27) Washida, N.; Martinez, R. I.; Bayes, K. D. *Z. Naturforsch. Jeil A* **1974**, *29*, 251–255.

(28) Shibuya, K.; Etaba, T.; Obi, K.; Tanaka, I. *J. Phys. Chem.* **1977**, *81*, 2292–2294.

(29) Rielly, J. P.; Clark, J. H.; Moore, C. B.; Pimentel, G. C. *J. Chem. Phys.* **1978**, *69*, 4381–4394.

(30) Nadtochenko, V. A.; Sarkisov, O. M.; Vedeneev, V. I. *Dokl. Akad. Nauk SSSR* **1979**, *244*, 152–156.

(31) Veyret, B.; Lesclaux, R. *J. Phys. Chem.* **1981**, *85*, 1918–1922.

(32) Gill, R. J.; Johnson, W. D.; Atkinson, G. H. *Chem. Phys.* **1981**, *58*, 29–44.

(33) Adachi, H.; Basco, N.; James, D. G. L. *Chem. Phys. Lett.* **1978**, *59*, 502–505.

(34) Parkes, D. A. *Chem. Phys. Lett.* **1981**, *77*, 527–532.

(35) McDade, C. E. *Diss. Abstr. Int. B* **1979**, *39*, 4373.

(36) McDowell, C. A.; Thomas, J. H. *Trans. Faraday Soc.* **1950**, *46*, 1030–1039.

(37) Pedler, A. E.; Pollard, F. H. *Trans. Faraday Soc.* **1957**, *53*, 44–50.

(38) Christie, M. I.; Voisey, M. A. *Trans. Faraday Soc.* **1967**, *63*, 2459–2463.

(39) Christie, M. I.; Voisey, M. A. *Trans. Faraday Soc.* **1967**, *63*, 2702–2707.

(40) Braun, W.; Rajbenbach, L.; Eirich, F. R. *J. Phys. Chem.* **1962**, *66*, 1591–1595.

(41) Vogt, T. C.; Hamill, W. H. *J. Phys. Chem.* **1963**, *67*, 292–295.

(42) Taylor, J. W.; Martin, J. C. *J. Am. Chem. Soc.* **1967**, *89*, 6904–6911.

(43) Skell, P. S.; May, D. D. *J. Am. Chem. Soc.* **1981**, *103*, 967–968.

during the photolysis of CF_2Cl_2. In our experiments it was not possible to determine whether CF_2 was produced directly as has been suggested by others,[45-49]

$$CF_2Cl_2 \xrightarrow{nh\nu} CF_2 + Cl_2 \tag{9}$$

or indirectly by secondary photolysis,

$$CF_2Cl \xrightarrow{nh\nu} CF_2 + Cl \tag{10}$$

The presence of CF_2 did not interfere with the reaction under study since this radical did not react to a measurable extent during the observation time following each laser pulse.

We were unable to directly monitor the extent of decomposition of CF_2Cl_2 by IRMPD following each laser pulse because the ionization potential of this molecule is higher than 11.6 eV, the most energetic ionizing radiation available in our PIMS. Therefore, we were unable to directly determine the Cl-atom concentration after laser photolysis. Following the conclusion of the major portion of our study, we discovered that reaction 2 is also an excellent Cl-atom source for this kind of experiment. The parent molecule, C_6F_5Cl, can be monitored with our detection system, and, therefore, the extent of decomposition by IRMPD can be measured directly. This second Cl-atom source will be used extensively in future studies. Based on the measured Cl-atom concentrations produced by reaction 2, we estimate that 1-3% of the CF_2Cl_2 decomposed during each laser pulse in our experiments (the estimates of CF_2Cl and CH_3CO concentrations given in the remainder of this paper assume a 2% decomposition of the precursor molecule).

Generation of Acetyl Radicals. When the flowing gas mixture containing CF_2Cl_2, CH_3CHO and He was irradiated, the chlorine atoms produced by reaction 1 or 2 reacted rapidly with the CH_3CHO. The $[CH_3CHO]$ which was employed ($\sim 5 \times 10^{14}$ cm^{-3}) was high enough to assure rapid ($\tau_{1/2} \approx 20$ μs) stoichiometric conversion of the Cl atoms to acetyl radicals by reaction 3.[50]

We verified that the radical produced was essentially exclusively CH_3CO (and not CH_2COH) by observing the possible radical products produced by the reaction,

$$Cl + CD_3CHO \rightarrow CD_3CO + HCl \tag{11}$$

No CD_2CHO was detected while CD_3CO was produced in easily observable amounts. This test confirms that the Cl atom abstracts primarily the aldehydic hydrogen of CH_3CHO.

The initial acetyl radical concentrations were chosen to be sufficiently low ($< 10^{11}$ cm^{-3}) that pseudo-first-order conditions were achieved in all experiments in which the radical reacted with NO_2 ($[NO_2] = 1\text{-}5 \times 10^{12}$ cm^{-3}) and to assure negligible radical loss by second-order radical recombination. The second-order recombination half-life at these low initial radical concentrations ($\tau_{1/2} \geq 500$ ms) is much longer than the first-order half-life when NO_2 is present (3-10 ms).[33,34] Homogeneous recombination is considered a negligible radical loss process at these low initial free-radical concentrations and is not included in the data reduction procedure.

In the absence of NO_2, CH_3CO decays exponentially with an apparent first-order rate constant of ~ 50 s^{-1} if the Pyrex reactor walls are clean but uncoated. If the walls are first cleaned with 5% ammonium bifluoride and then coated with boric acid, the radical loss rate is reduced to an apparent wall-loss rate constant, $k_w \approx 20$ s^{-1}. With the addition of increasing amounts of NO_2, a proportional increase in the decay constant of acetyl radicals was observed. Experiments were performed up to NO_2 concentrations which yielded a first-order decay constant of ~ 150 s^{-1}.

In these experiments there was essentially complete temporal isolation of all three kinetic processes: Cl-atom production ($\tau_{1/2} \approx 10^{-6}$ s), reaction to produce acetyl radicals ($\tau_{1/2} \approx 10^{-4}$ s), and reaction of acetyl radicals with NO_2 ($\tau_{1/2} = 4\text{-}40 \times 10^{-3}$ s).

Source and Purification of Reactants. Dichlorodifluoromethane (Matheson) and nitrogen dioxide (Matheson) were condensed at liquid nitrogen temperature, fractionally distilled, and stored as dilute mixtures in argon (Linde). Acetaldehyde (Aldrich) was purified by the freeze-pump-thaw method at liquid nitrogen temperature. Helium (Linde), argon (Linde), and CD_3CHO (Merck, 98 atom % D) were used without further purification.

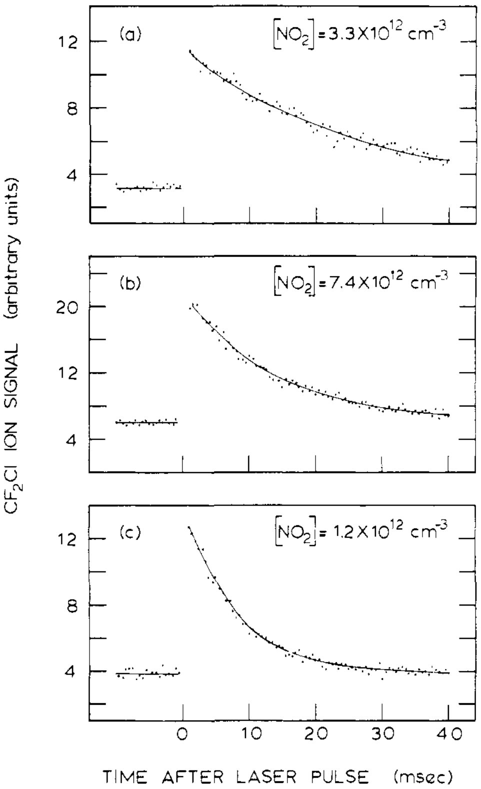

Figure 1. CF_2Cl ion signal decays as a function of $[NO_2]$. In all experiments $p = 2$ torr, fluence $\simeq 3$ J/cm^2, $[CF_2Cl]_0 \approx 8 \times 10^{10}$ cm^{-3}. (a) $[NO_2] = 3.3 \times 10^{12}$ cm^{-3}, $k_{exp} = 40$ s^{-1}; (b) $[NO_2] = 7.4 \times 10^{12}$ cm^{-3}, $k_{exp} = 73$ s^{-1}; (c) $[NO_2] = 1.24 \times 10^{13}$ cm^{-3}, $k_{exp} = 131$ s^{-1}.

Results

In this study we have determined the rate constants and the mechanism of both the $CF_2Cl + NO_2$ and $CH_3CO + NO_2$ reactions. Both CF_2Cl, which is produced directly during the IRMPD of CF_2Cl_2, and CH_3CO, which is produced by reaction 3, subsequently react with NO_2. To establish the two mechanisms, that of the $CF_2Cl + NO_2$ reaction was investigated first, since it can be studied without the second occurring concurrently by excluding acetaldehyde from the system. Experiments in which both reactions occurred simultaneously were then performed and the data analyzed to determine the mechanism of the $CH_3CO + NO_2$ reaction. The rate constants at ambient temperature for both reactions were also measured. The results of these studies and the data analysis are presented in this section.

Mechanism of the $CF_2Cl + NO_2$ Reaction. A gas mixture containing CF_2Cl_2 (0.03%), NO_2 (0.02%), and He (99.95%) at a total pressure of 1.0 torr was used to search for possible products. The only product ion signal detected following pulsed irradiation at ~ 3.5 J/cm^2 was NO. The growth of the NO ion signal was essentially a mirror image of that observed for the decay of the CF_2Cl ion signal, indicating that NO is an initial product of the $CF_2Cl + NO_2$ reaction. The failure to detect CF_2ClO, the other product produced with NO in reaction 5, was not unexpected. We have been unable to detect other alkoxy radicals, such as CH_3O, in other systems.[2] There is evidence from a mass spectrometric study using electron bombardment that detection sensitivity for alkoxyl radicals is unusually low.[51] The products which were monitored but which were not detected were CF_2 (11.6 eV), CF_2ClO (10.2 eV), CF_2ClNO_2 (11.6 eV), and $(CF_2Cl)_2$ (11.6 eV).[52] The photoionization energies used to detect and monitor

---

(44) Sudbø, Aa. S.; Schulz, P. A.; Grant, E. R.; Shen, Y. R.; Lee, Y. T. *J. Chem. Phys.* **1979**, *70*, 912-929.

(45) Hudgens, J. W. *J. Chem. Phys.* **1978**, *68*, 777-778.

(46) Folcher, G.; Braun, W. *J. Photochem.* **1978**, *8*, 341-354.

(47) King, D. S.; Stephenson, J. C. *J. Am. Chem. Soc.* **1978**, *100*, 7151-7155.

(48) Morrison, R. J. S.; Grant, E. R. *J. Chem. Phys.* **1979**, *71*, 3537-3538.

(49) Hill, G. A.; Grunwald, E.; Keehn, P. *J. Am. Chem. Soc.* **1977**, *99*, 6521-6526.

(50) Half-life estimated from Cl-atom rate constants given in Michael, J. V.; Nava, D. F.; Payne, W. A.; Stief, L. J. *J. Chem. Phys.* **1979**, *70*, 3652-3656.

(51) Hoyermann, K.; Loftfield, N. S.; Sievert, R.; Wagner, H. Gg. *Symp. (Int.) Combust. [Proc.]* **1981**, *18*, 831-844.

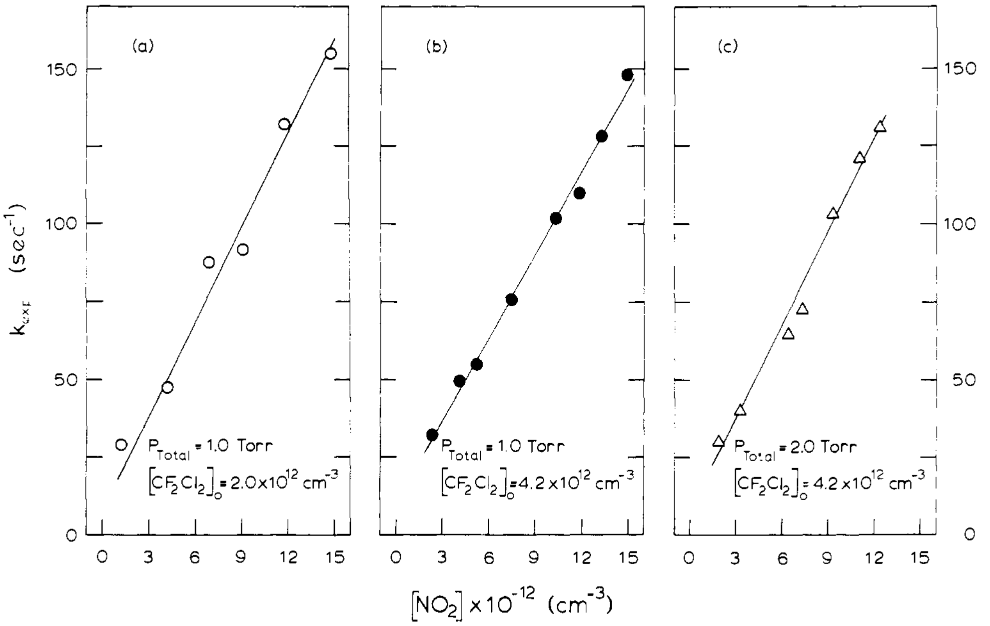

Figure 2. Results of experiments to determine k_5. For conditions of experiments, see Table I. k_5 value determined from the slopes of the lines are (a) 1.1×10^{-11}, (b) 8.9×10^{-12}, and (c) and 9.8×10^{-12} cm^3 molecule^{-1} s^{-1}.

species present were 10.2 eV for both NO and CF_2Cl.

From the results of these studies, we conclude that the $CF_2Cl + NO_2$ reaction proceeds either exclusively or nearly so by O-atom transfer, i.e., by reaction 5.

Rate Constant of the $CF_2Cl + NO_2$ Reaction. Three sets of experiments were performed in which the $CF_2Cl + NO_2$ rate constant at 295 ± 1 K was measured. Mixtures containing CF_2Cl_2, He, and various amounts of NO_2 were used in experiments in which the exponential decay of CF_2Cl was recorded following each laser pulse. Examples of measured CF_2Cl decay profiles are shown in Figure 1, and the results of the individual experiments are presented in Table I. In all experiments in which NO_2 was present, $[NO_2] >> [CF_2Cl]_0$ which assured pseudo-first-order conditions. The rate constant from each of the three sets of experiments was obtained from the slope of the line fitted through the points on a plot of the first-order decay constants vs. $[NO_2]$ (see Figure 2). The data-reduction procedure has been described in part 1.[1] The measured exponential decay constant changed by about a factor of 7 in each set of experiments, from an apparent $k_{wall} \approx 20$ s^{-1} when NO_2 was absent to $k_{exp} \approx 150$ s^{-1} when $[NO_2] \approx 1.5 \times 10^{13}$ cm^{-3}.

The three sets of experiments were performed to test whether the measured rate constant of reaction 5 depended on the total gas density or the initial CF_2Cl concentration. Each was varied separately by a factor of 2, the latter by increasing the concentration of the CF_2Cl precursor without increasing the laser fluence. No change in the rate constant with changes in these variables was apparent. The average value of k_5 from the three sets of experiments at 295 K is $k_5 = 9.6 \times 10^{-12}$ cm^3 molecule^{-1} s^{-1}. The estimated accuracy is ±20%.

Products of the $CH_3CO + NO_2$ Reaction. Two sets of experiments were performed to determine the products of the reaction of acetyl radicals with NO_2. Two CF_2Cl_2–CH_3CHO–NO_2–He gas mixtures at 1.0 torr total pressure were exposed to pulsed CO_2 laser radiation, and reactant and possible product ion signal profiles were recorded. In the first set, the reaction proceeded relatively slowly because a low NO_2 concentration was used ($[NO_2] = 2.1 \times 10^{12}$ cm^{-3}) while in the second the $CH_3CO + NO_2$ reaction proceeded more rapidly because a higher NO_2 concentration was employed ($[NO_2] = 6.7 \times 10^{12}$ cm^{-3}). In both sets of experiments the only apparent products detected, i.e., the only ion signals which increased following the initiation of the reaction, were those of CH_3 and NO. The actual ion signal profiles of reactant loss and product formation which were recorded in these experiments are shown in Figure 3. Possible products which were monitored but were not detected at a photoionization energy of 10.2 eV were CH_2CO, CH_3CO_2, HNO_2, and $CH_3CO_2NO_2$.

Table I. Initial Conditions and Experimental Results of $CF_2Cl + NO_2$ Rate Constant Measurements

p (torr)	$[CF_2Cl_2] \times 10^{-12}$ (cm^{-3})	approx $[CF_2Cl]_0 \times 10^{-10}$ (cm^{-3})	$[NO_2] \times 10^{-12}$ (cm^{-3})	k_{exp} (s^{-1})
1.0	2.0	4.0	2.3	29.
1.0	2.0	4.0	4.2	48.
1.0	2.0	4.0	6.9	88.
1.0	2.0	4.0	9.1	92.
1.0	2.0	4.0	11.8	132.
1.0	2.0	4.0	14.8	155.
$k_5 = 1.0 \times 10^{-11}$ cm^3 molecule^{-1} s^{-1}				
1.0	4.2	8.4	2.4	32.
1.0	4.2	8.4	4.1	50.
1.0	4.2	8.4	5.2	55.
1.0	4.2	8.4	7.5	76.
1.0	4.2	8.4	10.4	102.
1.0	4.2	8.4	11.9	110.
1.0	4.2	8.4	13.4	128.
1.0	4.2	8.4	15.0	148.
$k_5 = 8.9 \times 10^{-12}$ cm^3 molecule^{-1} s^{-1}				
2.0	4.2	8.4	1.9	30.
2.0	4.2	8.4	3.3	40.
2.0	4.2	8.4	5.5	65.
2.0	4.2	8.4	7.4	73.
2.0	4.2	8.4	9.4	103.
2.0	4.2	8.4	11.1	121.
2.0	4.2	8.4	12.4	131.
$k_5 = 9.8 \times 10^{-12}$ cm^3 molecule^{-1} s^{-1}				

The qualitative conclusions which can be drawn from these experiments is that the primary reaction of the CH_3CO radical and subsequent chemical reactions are clearly resolved and that CH_3 is a new product which appears as the acetyl radical reacts in the presence of NO_2. The CH_3 radical is also produced during the laser pulse (at $t = 0$) by the sensitized decomposition of CH_3CHO.[53] Since NO is also produced by both the $CF_2Cl + NO_2$ reaction and by a similar reaction of the CH_3 radicals,

$$CH_3 + NO_2 \rightarrow CH_3O + NO \qquad (12)$$

it is not apparent whether the NO concentration profile also

---

(52) Numbers in parentheses indicate photoionization energy used to detect or attempt to detect reactant or product.

[53] The initial production of CH_3 during the laser pulse did not occur when either CF_2Cl_2 or CH_3CHO was not in the system.

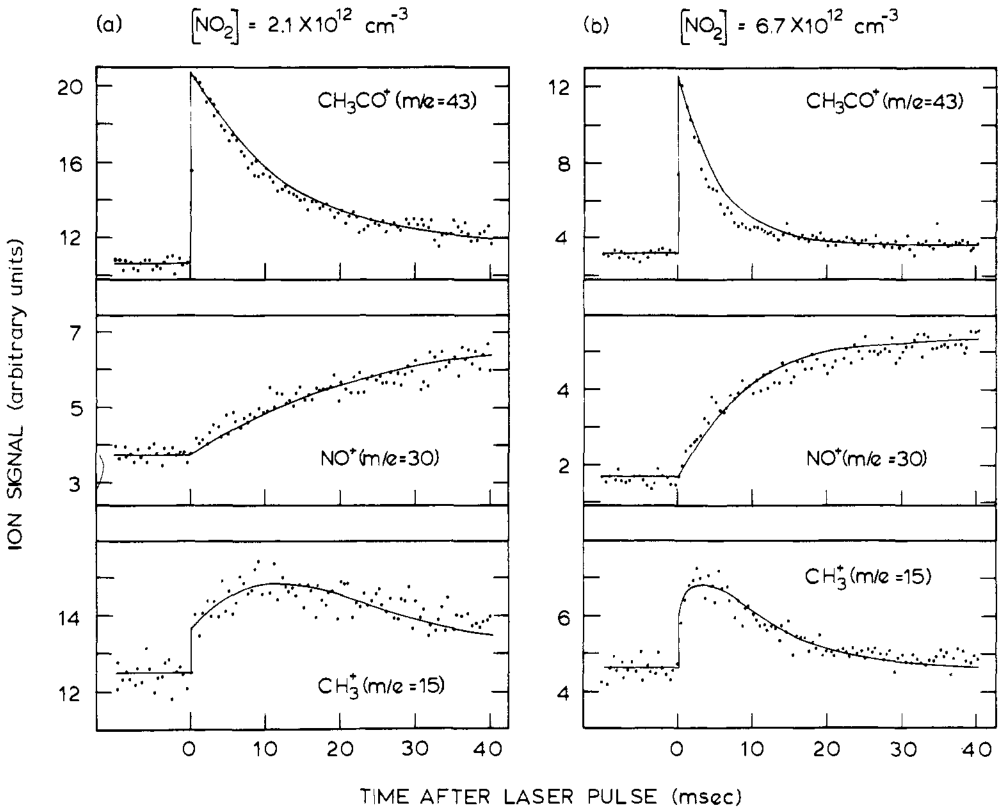

Figure 3. Reactant and product ion signal profiles in the $CH_3CO + NO_2$ reaction. In all experiments $P = 1$ torr, fluence ~ 3 J/cm^2. Initial conditions: (a) $[CF_2Cl_2] = 4.1 \times 10^{12}$ cm^{-3}, $[CH_3CHO] = 6.5 \times 10^{14}$ cm^{-3}, $[CH_3CO]_0 \sim 8.2 \times 10^{10}$ cm^{-3}, $[NO_2] = 2.1 \times 10^{12}$ cm^{-3}; (b) $[CF_2Cl_2] = 9.4 \times 10^{12}$ cm^{-3}, $[CH_3CHO] = 6.5 \times 10^{14}$ cm^{-3}, $[CH_3CO]_0 \sim 1.9 \times 10^{11}$ cm^{-3}, $[NO_2] = 6.7 \times 10^{12}$ cm^{-3}.

Table II. Initial Conditions and Experimental Results of $CH_3CO + NO_2$ Rate Constant Measurements

p (torr)	$[CF_2Cl_2] \times 10^{-12}$ (cm^{-3})	$[CH_3CHO] \times 10^{-14}$ (cm^{-3})	approx $[CH_3CO]_0 \times 10^{-10}$ (cm^{-3})	$[NO_2] \times 10^{-12}$ (cm^{-3})	k_{exp} (s^{-1})
1.0	1.8	5.7	3.6	0	18.
1.0	1.8	5.7	3.6	1.0	43.
1.0	1.8	5.7	3.6	2.1	74.
1.0	1.8	5.7	3.6	3.4	119.
1.0	1.8	5.7	3.6	4.0	124.
1.0	1.8	5.7	3.6	5.2	159.
		$k_4 = 2.7 \times 10^{-11}$ cm^3 molecule^{-1} s^{-1}			
1.0	0.96	6.5	1.9	0	17.
1.0	0.96	6.5	1.9	1.0	49.
1.0	0.96	6.5	1.9	1.0	47.
1.0	0.96	6.5	1.9	2.0	76.
1.0	0.96	6.5	1.9	3.1	90.
1.0	0.96	6.5	1.9	3.8	96.
1.0	0.96	6.5	1.9	3.9	102.
1.0	0.96	6.5	1.9	4.3	154.
1.0	0.96	6.5	1.9	4.9	139.
		$k_4 = 2.5 \times 10^{-11}$ cm^3 molecule^{-1} s^{-1}			
2.0	2.3	6.4	4.6	0	17.
2.0	2.3	6.4	4.6	0.9	42.
2.0	2.3	6.4	4.6	1.8	67.
2.0	2.3	6.4	4.6	2.9	83.
2.0	2.3	6.4	4.6	3.6	102.
2.0	2.3	6.4	4.6	4.4	123.
		$k_4 = 2.4 \times 10^{-11}$ cm^3 molecule^{-1} s^{-1}			

contains a contribution from the $CH_3CO + NO_2$ reaction. The identification of CH_3 as an initial product establishes that the acetyl-radical reaction with NO_2 proceeds by reaction 4, and the absence of other products, particularly CH_2CO, confirms that it is the dominant route.[36-39] The more quantitative mechanistic information which is contained in these ion signal profiles is discussed in the next section where kinetic models are used to simulate the recorded ion signal profiles of both products.

Rate Constant of the $CH_3CO + NO_2$ Reaction. Three sets of experiments were again performed in which the $CH_3CO + NO_2$ rate constant at 296 ± 1 K was measured. Mixtures containing CF_2Cl_2, CH_3CHO, He, and various amounts of NO_2 were pulse irradiated to initiate the reaction. Initial conditions were chosen to produce pseudo-first-order conditions in every experiment. Nitrogen dioxide was again always in great excess, and initial CH_3CO concentrations were always so low ($<10^{11}$ cm^{-3}) that recombination was a negligible alternate loss process. Exponential decay of acetyl radicals was observed in both the presence and absence of NO_2. The measured first-order decay constants, k_{exp}, are plotted in Figure 4 vs. the $[NO_2]$ in the corresponding experiment. The conditions of each experiment are presented in Table II. Rate constants for reaction 4 were obtained from the

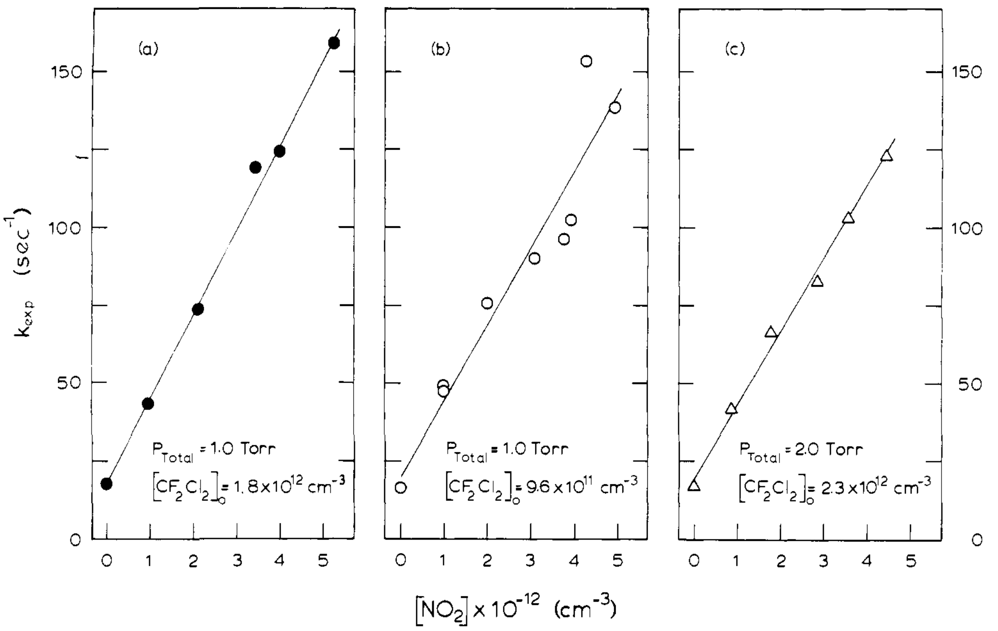

Figure 4. Results of experiments to determine k_4. For conditions of experiments, see Table II. k_4 values determined from the slopes of the lines are (a) 2.7×10^{-11}, (b) 2.5×10^{-11}, and (c) and 2.4×10^{-11} cm^3 molecule^{-1} s^{-1}.

plots shown in Figure 4 as discussed before.[1]

The three measured rate constants for reaction 4 are also essentially independent of the parameters which were varied in the three sets of experiments, total pressure and $[CH_3CO]$ (both changed by a factor of 2). The average value of k_4 obtained from these experiments is $k_4 = 2.5 \times 10^{-11}$ cm^3 molecule^{-1} s^{-1}. The estimated accuracy is ±25%.

Discussion

Use of Halogen Atoms To Generate Polyatomic Free Radicals. The indirect production of polyatomic free radicals through pulsed homogeneous production of Cl atoms by IRMPD followed by their rapid reaction with an organic molecule yielded *initial conditions* following the completion of the Cl-atom reaction which are suitable for performing direct time-resolved studies of the ensuing reactions of the polyatomic free radical. Since greater than 95% of the Cl-atom reaction occurs after the laser pulse, no significant photolysis of the polyatomic free radical produced by this reaction can occur. This indirect method of generating reaction intermediates is not only rapid but appears to be stoichiometric under the conditions of our experiments. The method will be used in the future for producing free radicals for similar studies involving other free radicals.

The principal disadvantage of the method involves the need to have relatively high concentrations of the free-radical precursor (e.g., CH_3CHO) present in the system to assure the rapid stoichiometric conversion of the chlorine atoms to the polyatomic free radicals. In our study CH_3CHO was essentially "inert" after the Cl-atom reaction occurred. However, in systems involving other free-radical precursors or in experiments conducted at elevated temperatures, the precursor may be more reactive and provide an undesired alternate reactive path in addition to the one under study.

A second disadvantage is that sensitized decomposition of the organic molecule used as the source of the polyatomic free radical does occur to an observable extent. The molecule directly excited, CF_2Cl_2, can apparently transfer enough internal energy to a small fraction of the CH_3CHO molecules to promote them to the quasi-continuum. In this activated state, they in turn can absorb additional photons and dissociate,

$$CH_3CHO^* + nh\nu \rightarrow CH_3 + HCO \qquad (13)$$

Such processes have been observed in other systems.[54] In our study, only a very small amount of CH_3CHO dissociated during the laser pulse (~0.01%), and the radicals produced did not significantly increase the complexity of the data analysis.

A limitation of the procedure is caused by the fact that H-atom abstraction by chlorine atoms becomes increasingly unselective as the organic molecule becomes larger and more complex.[55] These Cl-atom reactions can produce a mixture of free radicals, all of the same mass number (M - 1), which would cause difficulty in interpreting the observations of the ensuing reactions if they are monitored by mass spectrometry. In selected instances, however, this *problem* may be used to advantage to produce isomers of the same radical for separate studies of their reactions. For example, $\cdot CH_2CHO$ and $CH_3\dot{C}O$ can be separately produced by different halogen-atom reactions. The H-atom abstraction reactions involving fluorine atoms are known to be almost completely unselective.[56] Thus, the reaction of fluorine with CH_3CHO would produce a mixture of isomers which, however, would be (~75%) the vinyloxy radical. On the other hand, Cl-atom abstraction reactions with organic molecules tend to favor abstraction of the more weakly bound hydrogens.[57] The essentially exclusive production of acetyl radicals by the Cl + CH_3CHO reaction is one example. Another is the Cl + CH_3OH reaction, which proceeds almost exclusively by removal of the H atom bound to carbon (C–H bond energy = 95 kcal/mol) to yield the hydroxymethyl radical,[57,58]

$$Cl + CH_3OH \rightarrow CH_2COH + HCl$$

The O–H bond in methanol (O–H bond energy = 104 kcal/mol) is significantly stronger than the C–H bonds.

Kinetic Modeling of the $CH_3CO + NO_2$ Reaction. Using a kinetic model to simulate the $CH_3CO + NO_2$ experiments, we have calculated temporal ion-signal profiles for the six reactant and product ion signals which are shown in Figure 3. The lines drawn through the data sets are the analytical solutions of the appropriate rate equations which are discussed below. In order to assess our understanding of the kinetics of this system and to determine how accurately the product ion-signal profiles reflect the actual product concentration profiles in the tubular reactor, we have used only rate constants for the presumed elementary reactions in this modeling exercise which were actually measured

---

(54) Karve, R. S.; Sarkar, S. K.; Rama Rao, K. V. S.; Mittal, J. P. *Chem. Phys. Lett.* **1981**, *78*, 273–276.

(55) Knox, J. H.; Nelson, R. L. *Trans. Faraday Soc.* **1959**, *55*, 937–946.

(56) Dill, B.; Heydtmann, H. *Chem. Phys.* **1980**, *54*, 9–20.

(57) See reference cited in footnote 50.

(58) Radford, H. E. *Chem. Phys. Lett.* **1980**, *71*, 195–197.

under pseudo-first-order conditions, either in this study or a previous one.[2] The only adjustable parameter which occurs in each analytical expression for species concentration is a multiplicative scaling constant which relates the measured ion signal to calculated species concentration.

In both sets of experiments shown in Figure 3 significantly higher initial CH_3CO concentrations were used than were later used to measure the rate constant of the $CH_3CO + NO_2$ reaction. These higher CH_3CO concentrations were needed to produce the higher product concentrations which were required to obtain product ion signal profiles of a quality which would be suitable for quantitative modeling. At these elevated CH_3CO concentrations, homogeneous radical recombination was no longer a completely insignificant acetyl–radical loss process, particularly in the set of experiments using the higher NO_2 concentration. Since the initial CH_3CO concentrations in these experiments were not accurately known, the recombination reaction could not be included in the kinetic model without introducing a second adjustable parameter. We decided not to include the recombination process in the analysis.

In the set of experiments using the lower NO_2 concentration, the CH_3CO concentration was only slightly elevated ($[CH_3CO]_0 \approx 8.2 \times 10^{10}$ cm^{-3}) and recombination was almost insignificant. However, in the set of experiments using the higher NO_2 concentration, the initial CH_3CO concentration was significantly elevated ($[CH_3CO]_0 \approx 1.9 \times 10^{11}$ cm^{-3}) and the neglect of recombination is definitely noticeable. The products produced by recombination are stable ($(CH_3CO)_2$ or $CH_2CO + CH_3CHO$) and do not react further under the conditions of these experiments.

The kinetic model which was used assumes instant conversion of Cl atoms to CH_3CO, initial CH_3 production during the laser pulse, and the following reactions:

$$CH_3CO + NO_2 \rightarrow (CH_3 + CO_2) + NO \quad (4)$$

$$CF_2Cl + NO_2 \rightarrow CF_2ClO + NO \quad (5)$$

$$CH_3 + NO_2 \rightarrow CH_3O + NO \quad (12)$$

$$CH_3CO \rightarrow \text{wall destruction} \quad (14)$$

$$CF_2Cl \rightarrow \text{wall destruction} \quad (15)$$

$$CH_3 \rightarrow \text{wall destruction} \quad (16)$$

The rate constants k_4 and k_5 are given in the text, k_{12} and k_{16} were measured previously,[2] and k_{14} and k_{15} (40 and 20 s^{-1}, respectively) were measured on the day the experiments in Figure 3 were performed. From the stoichiometry of the initial rapid reaction, $[CH_3CO]_0 = [CF_2Cl]_0$.

CH_3CO Profiles. The CH_3CO loss is presumed to be due only to reaction with NO_2 and to a wall reaction. Conditions are pseudo first order. The resulting exponential function for CH_3CO loss is plotted in Figure 3. The scaling constant was chosen to obtain agreement at $t = 0$. The ion signal profiles are corrected for a contribution due to fragmentation in the ion source of $(CH_3CO)_2$ which is produced by the minor amount of CH_3CO recombination which occurs in the system. These CH_3CO ion-signal profiles were also monitored in other experiments at lower initial CH_3CO concentrations to measure the rate constants used in the model. Therefore, the deviation of the calculated profiles from those which were measured in an indication of the importance of the CH_3CO recombination reaction in these experiments. A comparison of measured and calculated profiles in Figure 3 indicates a small, almost negligible recombination contribution in the experiment designated (a) and a significant contribution in the one labeled (b).

CH_3 Profiles. The CH_3 radical is presumed to be produced by the $CH_3CO + NO_2$ reaction and to subsequently react with NO_2 or be lost in a first-order wall process. Since conditions are first order or pseudo first order for all the CH_3 reactions, the reaction mechanism is essentially two consecutive first-order reactions. The analytical solution for such a system is given in standard texts.[59,60] The scaling constant was chosen to obtain agreement at the concentration maximum. The calculation requires knowledge of the initial CH_3 concentration produced at $t = 0$ by the photosensitized decomposition of CH_3CHO. Since there is an adjustable scaling constant, only $[CH_3CO]_0/[CH_3]_0$ is actually required. This ratio was determined to be 3 based on the observed $[CH_3]_{max}/[CH_3]_0$ ratio and the values of t_{max}, the time needed to reach the maximum CH_3 concentration.[59]

Both calculated temporal profiles simulate the measured CH_3 concentration profiles very closely. There was at least a theoretical possibility that the CH_3^+ ion signal which grew as reaction proceeded was a fragment ion of a stable CH_3CO_2 product.[43] The close agreement between calculated and measured CH_3 profiles using the known reactivity of CH_3 in this system essentially eliminates this possible alternate interpretation of these experiments.

NO Profiles. In this system NO is produced by three primary processes, by the reactions of CH_3CO, CF_2Cl, and CH_3 which are present at $t = 0$, and by the secondary reaction of the CH_3 radicals produced by reaction 4. The analytical expression for the total NO concentration in the system from the two parallel routes is easily obtained.[59,60] In this case the scaling constant was chosen to obtain agreement with the measurements at 40 ms.

The calculated NO concentration profiles again agree well with the measurements. The small deviations are qualitatively in the direction which would be expected if recombination were depleting the acetyl radicals to a noticeable extent. When the calculation is repeated excluding reaction 4 as an NO source, and the new calculated NO profiles are rescaled at 40 ms, the agreement with experiment is also very good. The shape of the NO profile is not significantly altered by removal of one of the three NO sources. Therefore, these measured NO profiles do not establish that NO is produced in reaction 4. The evidence for the mechanism of the $CH_3CO + NO_2$ reaction remains the identification of CH_3 as a product and the absence of CH_2CO which can be easily detected by our PIMS.

From the close agreement between the recorded ion signals and the calculated ones, we conclude that the mechanism proposed for this system is correct and that it, together with the rate constants obtained in this study, provides a quantitative understanding of the kinetics of the $CH_3CO + NO_2$ reaction. It is also apparent from these and earlier experiments that our experimental method provides very quantitative representations of not only reactant, but also of intermediate and product concentration profiles in the reactor used in these studies.

Mechanisms of $R + NO_2$ Reactions. We have now studied four $R + NO_2$ reactions, two in prior investigations and two here. In all instances the reaction was observed to proceed predominantly, if not exclusively, by O-atom transfer from NO_2 to the polyatomic free radical. Primary products were detected in all of the investigations. The observation that CH_3 is a product of the $CH_3CO + NO_2$ reaction is a direct confirmation of reaction 4 as the mechanism of this reaction. The shape of the CH_3^+ ion signal profiles was well simulated by a mechanism which included the instantaneous decomposition of the acetoxy radical produced in reaction 4 to yield $CH_3 + CO$. This latter agreement supports the suggested instability of this reaction intermediate.[36-43]

In future studies, we shall investigate the mechanisms of the reactions of more complex organic free radicals with NO_2. For alkyl radicals containing more than one carbon atom, a second reactive route is also likely to occur,

$$R'CH_2CH_2 + NO_2 \rightarrow R'CH{=}CH_2 + HNO_2 \quad (17)$$

The production of olefins during the photooxidation of isobutane by NO_2 has been cited as due in part to reaction 17.[61] There have not as yet been any quantitative studies of larger hydrocarbon radicals with NO_2. In cases where both possible routes, O-atom

---

(59) Benson, S. W. "The Foundations of Chemical Kinetics"; McGraw-Hill: New York, 1960; p 33.

(60) Moore, J. W.; Pearson, R. G. "Kinetics and Mechanism"; Wiley: New York, 1981; p 290.

(61) Paraskevopoulos, G.; Cvetanović, R. J. *J. Phys. Chem.* **1977**, *81*, 2598–2601.

and H-atom transfer, occur to a significant extent, it will be possible to directly measure the extent to which the reaction proceeds by each of the two oxidation mechanisms.

Rate Constants of R + NO_2 Reactions. The two R + NO_2 reactions investigated in this study as well as the two which were studied earlier proceed extremely rapidly. The rate constants for the reactions of the three hydrogen-containing radicals (CH_3, C_3H_5, and CH_3CO) with NO_2 at ambient temperature are between 2.5 and 4 × 10^{-11} cm^3 $molecule^{-1}$ s^{-1}. This corresponds to a thermally averaged cross section at 300 K of between 3 and 7 $Å^2$. None of these reactions could, therefore, have a significant barrier to reaction (E_a must be less than 1 kcal/mol).

The reaction of the perhalogenated radical with NO_2 is distinctly slower (by a factor of 3) than the other three reactions studied. Halogen substitution is known to reduce the reactivity of hydrocarbon free radicals. For example, the CF_3 + NO_2 rate constant at 300 K is a factor of 10 less than that of the CH_3 + NO_2 reaction.[4]

There have been no prior measurements of the rate constants of reaction 4 or 5.[62]

The modeling of the kinetics of both the thermal and the photochemical nitration of hydrocarbons requires quantitative information on R + NO_2 reactions.[61,63,64] The importance of the direct O-atom transfer route has heretofore been either underestimated or not taken into account in a quantitative manner owing to a prior lack of mechanistic and kinetic information on this general type of reaction. The results of this study provide new quantitative information for obtaining a better understanding of the oxidation of hydrocarbons by NO_2.

Acknowledgment. This reasearch was supported by the Department of Energy, Office of Basic Energy Sciences, under Contract No. DE-AC02-78ER14593. We wish to thank Mr. Paul Sawyer for developing the computer codes for our data acquisition and analysis.

---

[62] An indirect determination of $k(CH_3CO + NO_2)/k(CH_3CO + NO)$ has been reported (see ref 38).

[63] Ballod, A. P.; Shtern, V. Ya. *Usp. Khim.* **1976**, *45*, 1428–1460.

[64] Umsted, M. E.; Fleming, J. W.; Lin, M. C. *IEEE J. Quantum Electron.* **1980**, *QE-16*, 1227–1229.

Bifurcated Hydrogen Bond and Large Amplitude Vibrations in Glycine Methyl Ester

Walther Caminati* and Rinaldo Cervellati

Contribution from Istituto Chimico "G. Ciamician", Università di Bologna, 2-I-40126 Bologna, Italy, and Istituto di Spettroscopia Molecolare del C.N.R., 1-I-40126 Bologna, Italy.

Received December 28, 1981

Abstract: The rotational spectrum of glycine methyl ester has been studied in order to investigate the nature of its hydrogen bond and its large amplitude motions. The moments of inertia of the normal, NHD, and ND_2 isotopic species indicate that the molecule has a plane of symmetry which contains all the heavy atoms and an internal bifurcated hydrogen bond in which the amino group chelates the carbonyl oxygen. From an analysis of the A–E splittings in the ground vibrational state, the methyl barrier to internal rotation has been determined to be $V_3 = 1177 \pm 30$ cal/mol. The rotational spectra of some vibrational satellites have been also assigned.

1. Introduction

The study of internal hydrogen bonding by microwave spectroscopy (MWS) has supplied information for small systems as small as the isolated molecules in the gas phase (see, for example, ref 1–8 and references therein). However, few molecules with a N—H···O internal hydrogen bond, the most common kind in biological systems, have been investigated in this way. 2-Methoxyethylamine,[1] where only the conformation stabilized by the internal hydrogen bond has been detected, was the first one studied.

The more stable conformation of glycine (GLY), the smallest amino acid, presents an internal bifurcated hydrogen bond:[2]

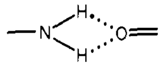

but two previous studies with MWS detected a conformer displaying a hydrogen bond of the type O—H···N.[3,4] This kind of hydrogen bond appears to be preferred with respect to the N—H···O one in 2-aminoethanol,[5] alaninol and 1-amino-2-propanol,[6] 2-methylaminoethanol,[7] and 3-aminopropanol.[8]

Some time ago, when we were aware only of the results of ref 3 and 4, we decided to study the methyl ester of glycine (GME), where the methyl group replacing the hydroxyl hydrogen inhibits the formation of the O—H···N hydrogen bond, in order to obtain a molecular system with a N—H···O internal hydrogen bond. After we had obtained a great deal of information on GME, a second paper by Suenram and Lovas on GLY appeared.[2] They reported the microwave spectrum of the conformation with the internal bifurcated hydrogen bond and stated this second conformer to be about 0.5 kcal mol^{-1} more stable than the conformer reported in ref 3 and 4. Nevertheless, we completed our study on GME, which is (with respect to the hydrogen bonding) a more simple system. Furthermore, the study of the large amplitude internal motions like those of the methyl group and the two heavy atom skeletal torsions is of interest in order to obtain information about the corresponding potential surfaces and the possible tor-

---

[1] Caminati, W.; Wilson, E. B. *J. Mol. Spectrosc.* **1980**, *81*, 356–372.

[2] Suenram, R. D.; Lovas, F. J. *J. Am. Chem. Soc.* **1980**, *102*, 7180–7184.

[3] Brown, R. D.; Godfrey, P. D.; Storey, J. W. V.; Bassez, M. P. *J. Chem. Soc., Chem. Commun.* **1978**, 547–548.

[4] Suenram, R. D.; Lovas, F. J. *J. Mol. Spectrosc.* **1978**, *72*, 372–382.

[5] Penn, R. E.; Curl, R. F., Jr. *J. Chem. Phys.* **1971**, *55*, 651–658.

[6] Ellingsen, B. H.; Marstokk, K. M.; Møllendal, H. *J. Mol. Struct.* **1978**, *48*, 9–23. Marstokk, K. M.; Møllendal, H. *Ibid.* **1976**, *35*, 57–66.

[7] Penn, R. E.; Buxton, L. W. *J. Mol. Spectrosc.* **1975**, *56*, 229–238.

[8] McMahan, M. A.; Sharma, S. D.; Curl, R. F., Jr. *J. Mol. Spectrosc.* **1979**, *75*, 220–233.

0002-7863/82/1504-4748$01.25/0